Journal of Immunological Methods 475 (2019) 112684

Contents lists available at ScienceDirect

Journal of Immunological Methods

journal homepage: www.elsevier.com/locate/jim

Review

Immunophenotypic dissection of normal hematopoiesis

Alberto Orfao[a,c,*], Sergio Matarraz[a,c], Martín Pérez-Andrés[a,c], Julia Almeida[a,c], Cristina Teodosio[b], Magdalena A. Berkowska[b], Jacques J.M. van Dongen[b], on behalf of EuroFlow

[a] Cancer Research Center (IBMCC, USAL-CSIC), Cytometry Service (NUCLEUS) and Department of Medicine, University of Salamanca, Salamanca, Spain
[b] Department of Immunohematology and Blood Transfusion, Leiden University Medical Center, Leiden, Netherlands.
[c] Institute of Biomedical Research of Salamanca (IBSAL), Centro de Investigación Biomédica en Red de Cáncer (CIBERONC), Salamanca, Spain

ARTICLE INFO

Keywords:
Immunophenotype
Flow cytometry
Bone marrow
Peripheral blood
Hematopoiesis
Lymphoid maturation
Myeloid maturation

ABSTRACT

Flow cytometry immunophenotyping is essential for diagnosis, classification and monitoring of clonal hematopoietic diseases, particularly of hematological malignancies and primary immunodeficiencies. Optimal use of immunophenotyping for these purposes requires detailed knowledge about the phenotypic patterns of normal hematopoietic cells.

In the past few decades, flow cytometry has benefited from technological developments allowing simultaneous analysis of multiple antigen stainings with ≥3–35 distinct fluorochrome-conjugated antibodies for increasingly higher numbers of cells. These advances have contributed to expand our knowledge about the phenotypic differentiation profiles of normal hematopoietic cells, from uncommitted $CD34^+$ precursors in the bone marrow (BM) and peripheral blood (PB), to the several hundreds of populations of circulating myeloid and (B and T) lymphoid cells identified so far. Detailed dissection of the normal phenotypic profiles of hematopoietic cells has settled the basis for identification of aberrant phenotypes on leukemia and lymphoma cells. Thus, it has contributed to: i) more sensitive identification of leukemia/lymphoma cells (especially when represented at low frequencies in a sample), and ii) more accurate classification of hematological malignancies. In this manuscript, we review the major phenotypic features of hematopoietic cells, from the more immature BM $CD34^+$ precursors committed to the myeloid and lymphoid lineages toward mature hematopoietic cells circulating in PB (e.g. neutrophils, monocytes, basophils, eosinophils, dendritic cells, erythroid cells, and B- and T-cells) and those homing to other tissues (e.g. plasma cells, mast cells).

1. Introduction

Since the earliest immunophenotypic studies (Loken et al., 1987a; Loken et al., 1987b), important advances have been achieved on our understanding of the immunophenotypic patterns of normal hematopoietic cells in BM, PB and to a lesser extent also, in lymph nodes and other lymphoid tissues. To a large extent these advances have been linked to the introduction and use of multiparameter flow cytometry (MFC) immunophenotyping, which allows simultaneous quantitative analysis of multiple features of hundreds to millions of individual cells in a relatively short time (Orfao et al., 1999). Currently available digital flow cytometers have incorporated multiple innovations by assembling additional lasers and adapted innovative detectors and optical configurations into instruments containing improved fluidics and up-to-date (sensitive and fast) electronics (Chattopadhyay et al., 2014). The development of new fluorochromes (Chattopadhyay and Roederer, 2012) and spectral detectors has further expanded the analytical potential of flow cytometry instruments (Chattopadhyay and Roederer, 2012; Flores-Montero et al., 2017; Theunissen et al., 2017a). Simultaneous assessment of multiple (e.g. ≥8-color) stainings in a sample aliquot based on comprehensive antibody combinations, significantly reduces the volume of sample required and the burden of sample preparation work and data acquisition time, compared to conventional multiple-sample aliquot stainings. Altogether, these advances have contributed to more precise i) identification and characterization of the distinct cell populations coexisting in a sample, ii) establishment of the precise relationship among them and, iii) discrimination between normal and tumor maturation pathways. In addition, ex vivo flow cytometry-based phenotypic studies of human hematopoiesis have also contributed to highlight and delineate differences with well-established in vitro and animal models. This has further contributed to a better understanding of the normal vs. altered phenotypic patterns of differentiation of

* Corresponding author at: Cancer Research Center (IBMCC, USAL-CSIC), Cytometry Service (NUCLEUS) and Department of Medicine, University of Salamanca, Salamanca, Spain.
E-mail address: orfao@usal.es (A. Orfao).

https://doi.org/10.1016/j.jim.2019.112684
Received 27 March 2019; Received in revised form 9 October 2019; Accepted 10 October 2019
Available online 30 October 2019
0022-1759/

human myeloid and lymphoid cells, and their fluctuations during life (Mello et al., 2017; Westers et al., 2017; Theunissen et al., 2017b; Blanco et al., 2018). Finally, flow cytometric analysis of normal hematopoietic cells have contributed to highlight the tight regulation of protein expression levels that single cells are subjected to during their maturation (Loken et al., 1987a; Loken et al., 1987b; Blanco et al., 2018).

Despite the multiple advantages of multicolor flow cytometry, simultaneous evaluation of multiple markers in a single flow cytometry measurement is also associated with greater technical complexity due to e.g. more complex fluorochrome compensation and data set matrices. Thereby, novel multivariate data analysis algorithms and graphical tools had to be developed and implemented in flow cytometry software programs (Pedreira et al., 2013; Kalina et al., 2012; van Dongen et al., 2012). In parallel, reference databases of well-defined samples/cases have also been constructed for fast automated gating of the many distinct cell populations contained in a flow cytometry data file (Flores-Montero et al., 2017; Pedreira et al., 2013; Lhermitte et al., 2018; Pedreira, 2012), further extending the need for new data visualization tools. Of note, such new graphics and graphical scale representations (linear vs. log vs. biexponential scales) are just visualization tools that do not affect the original data, e.g. they are used for data representation without modifying the actually measured values.

Here, we review the phenotypic characteristics of normal hematopoietic precursors and maturing cells of distinct lineages, based on their immunophenotypic profiles in primary human BM, PB and, to a lesser extent also the thymus and secondary lymphoid tissues (e.g. lymph nodes and/or spleen). Furthermore, we highlight the impact of these studies on the identification and characterization of altered phenotypic profiles associated with clonal hematological disorders and primary immunodeficiencies. Despite the markers here mentioned are based to a large extent on EuroFlow panels designed for identification and characterization of the distinct hematopoietic cell compartments (van Dongen et al., 2012), other alternative marker combinations might also be used.

2. Immunophenotypic features of CD34$^+$ hematopoietic stem cells and other CD34$^+$ precursors in BM and PB

Overall, two main compartments of CD34$^+$ cells are detected in normal human BM: i) a major population of CD34$^+$ hematopoietic *stem* and precursor cells (HPC) lacking CD73 expression and, ii) a minor population of endothelial cells with a CD34$^+$ CD10$^-$ CD73^{het} and CD81^{hi} phenotype (Smadja et al., 2007; Angelos et al., 2018) (Fig. 1A–C). CD34$^+$ HPC only represent a minor proportion (around 1%) of all BM nucleated cells. This compartment includes both CD34$^+$ uncommitted precursors and CD34$^+$ precursors with phenotypic evidence of early commitment toward distinct myeloid and lymphoid cell lineages (Matarraz et al., 2008) (Fig. 1D). Although the vast majority of CD34$^+$ HPC reside in BM, a minor fraction of (mostly uncommitted) CD34$^+$ HPC circulate in PB (< 0.1%) (Matarraz et al., 2018). From there, they migrate into BM niches in order to maintain homeostatic HPC levels across the entire organism. Of note, most normal CD34$^+$ cells in PB show an immature phenotype and only a minority of them display phenotypic evidence of commitment toward different myeloid and lymphoid cell lineages (Mayado et al., 2018). Briefly, these include CD34$^+$ precursors committed to: the mast cell (i.e. CD45^{int} CD34$^+$ CD117^{hi} HLA-DR$^{-/int}$ CD203c$^+$) and neutrophil lineages (CD45$^{lo/int}$ CD34$^+$ CD117$^+$ HLA-DR^{int} cyMPO$^+$ nuTdT$^-$ CD19$^-$), plasmacytoid and other dendritic cell compartments (pDC; CD45^{int} CD34$^+$ CD117$^+$ CD123$^{int/hi}$ HLADR^{hi} CD203c$^-$ and CD100$^+$) and the B-lymphoid lineage (CD45$^{lo/int}$ CD34$^+$ CD117$^-$ HLA-DR^{int} CD19$^+$ nuTdT$^+$) (Mayado et al., 2018; Collin and Bigley, 2018).

In contrast to PB CD34$^+$ HPC, uncommitted CD34$^+$ cells only represent < 10% of all CD34$^+$ cells in BM (Table 1). These uncommitted BM CD34$^+$ HPC show a CD34^{hi} CD38^{lo} CD71^{lo} HLADR$^+$ CD117$^+$ CD133^{hi} CD33$^+$ and CD13$^+$ phenotype, in the absence of other lymphoid-associated (e.g. CD19$^-$ CD7$^-$ CD56$^-$ nuTdT$^-$) and myeloid-related markers -e.g. cytoplasmic (cy)MPO$^-$, eosinophil peroxidase (cyEPO$^-$), CD11b$^-$ CD15$^-$ CD16$^-$ CD35$^-$ CD36$^-$ CD41$^-$ CD42a$^-$ CD61$^-$ CD64$^-$ CD71^{lo} CD105$^-$ CD123^{lo} CD203c$^-$ (Matarraz et al., 2008; Matarraz et al., 2010). Subsequent maturation of uncommitted precursors into different hematopoietic cell lineages is associated with expression of unique phenotypic patterns (characteristic for the myeloid and lymphoid lineages) as summarized in Table 1. Hence, > 90% of all BM CD34$^+$ HPC show phenotypic traits of differentiation (Matarraz et al., 2008; Matarraz et al., 2010). Maturation engagement of HPC in normal adult BM predominantly involves the erythroid (CD34$^+$ CD105$^+$ CD36$^+$), neutrophil (CD34$^+$ cyMPO$^+$), and B-lymphoid lineages (CD34$^+$ nuTdT$^+$) with a median of 35%, 33% and 23% of all CD34$^+$ hematopoietic cells, respectively (Matarraz et al., 2008; Matarraz et al., 2010) (Table 1).

Previous in vitro and in vivo (animal model) experiments based on relatively limited number of markers, have identified up to seven functionally distinct compartments of BM hematopoietic stem cells and multipotent progenitors, that also include CD34$^{-/low}$ cell fractions (Oguro et al., 2013). These consist of: i) multipotent uncommitted precursors (i.e. CD34$^+$ CD10$^-$ CD38$^-$ CD90$^-$ CD45RA$^-$), ii) common-myeloid precursors (CD34$^+$ CD10$^-$ CD38$^+$ CD123^{int} CD45RA$^-$), and also iii) lymphoid precursors (CD34$^+$ CD10$^+$), including iv) early lymphoid committed progenitors (CD34$^+$ CD10$^-$ CD38$^-$ CD90$^-$ CD45RA$^+$ and, v) erythroid/megakaryocytic precursors (CD34$^+$ CD10$^-$ CD38$^+$ CD123$^-$ CD45RA$^-$) (Oguro et al., 2013; Goardon et al., 2011; Majeti et al., 2007; Manz et al., 2002; Busch et al., 2015).

Further commitment of BM CD34$^+$ precursors to the erythroid lineage is associated with early expression of endoglin (CD105), CD35 (complement receptor-1; CR-1), CD44 (Laranjeira et al., 2015), and the thrombospondin receptor (CD36) (Fig. 1D–E). This is followed by an increase in cell surface membrane expression of the transferrin receptor (CD71) and glycophorin A (CD235a) (Westers et al., 2017; Matarraz et al., 2008; Matarraz et al., 2010; Laranjeira et al., 2015; Machherndl-Spandl et al., 2013) (Table 1). In turn, differentiation of CD34$^+$ cells toward the neutrophil lineage is associated with progressively higher expression of cyMPO$^{lo/hi}$ (Fig. 1E) CD13$^{+/hi}$ and CD33$^{+/hi}$ (Fig. 2B), followed by acquisition of CD15$^{-/+}$ and CD65$^{-/+}$. In parallel, early neutrophil precursors, sequentially downregulate CD34, CD117 and HLADR, associated with a slight decrease of CD45 levels (Fig. 2B) (Matarraz et al., 2008; Matarraz et al., 2010). More mature neutrophil precursors display an increase in their cytoplasmic complexity, as reflected by gradually increased sideward light scatter (SSC) (Fig. 2B) (Matarraz et al., 2008; Matarraz et al., 2010). These neutrophil precursor-associated profiles contrast with the phenotypic patterns of monocytic lineage-committed CD34$^+$ cells. Thus, early CD34$^+$ monocytic precursors represent around 20–25% of all CD34$^+$ cells in BM. Despite maintaining expression of CD13 and CD33, these monocytic precursors display an early CD34$^+$ HLADR$^+$ CD117$^+$ CD45$^+$ phenotype, associated with heterogeneous reactivity for CD64$^{+/hi}$ (Mello et al., 2017; Matarraz et al., 2008; Matarraz et al., 2010; Matarraz et al., 2017) and cyMPO$^{-/het}$ (Table 1; Fig. 1E). During early phases of hematopoietic cell development, monocytic precursors also upregulate CD11b, CD11c, cyCD68 and cyLysozyme expression. Further transition of monocytic precursors to more advanced maturation stages is associated with loss of CD34 expression and a slight downregulation of cyMPO (CyMPO^{lo}) (Mello et al., 2017; Matarraz et al., 2008; Matarraz et al., 2017). However, it should be noted that these "early monocytic phenotypes" might vary among healthy subjects. Hence, some healthy individuals show a well-defined subset of precursors with a HLADR^{hi} and cyMPO$^+$ phenotype, associated with lower expression of CD117 in the absence of CD64. The precise nature and identity (i.e. monocytic vs. other cell lineage) of such precursors remains to be fully elucidated.

In addition to the neutrophil, monocytic and erythroid precursors, a fraction of BM CD34$^+$ HPC also show phenotypic commitment to other

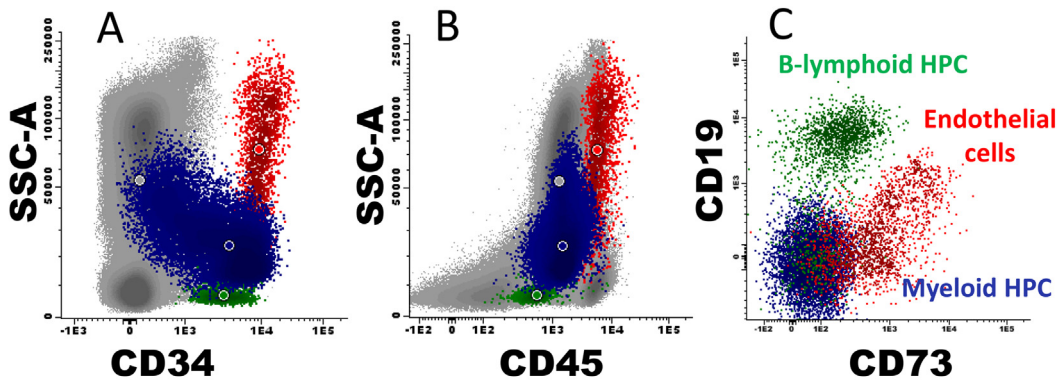

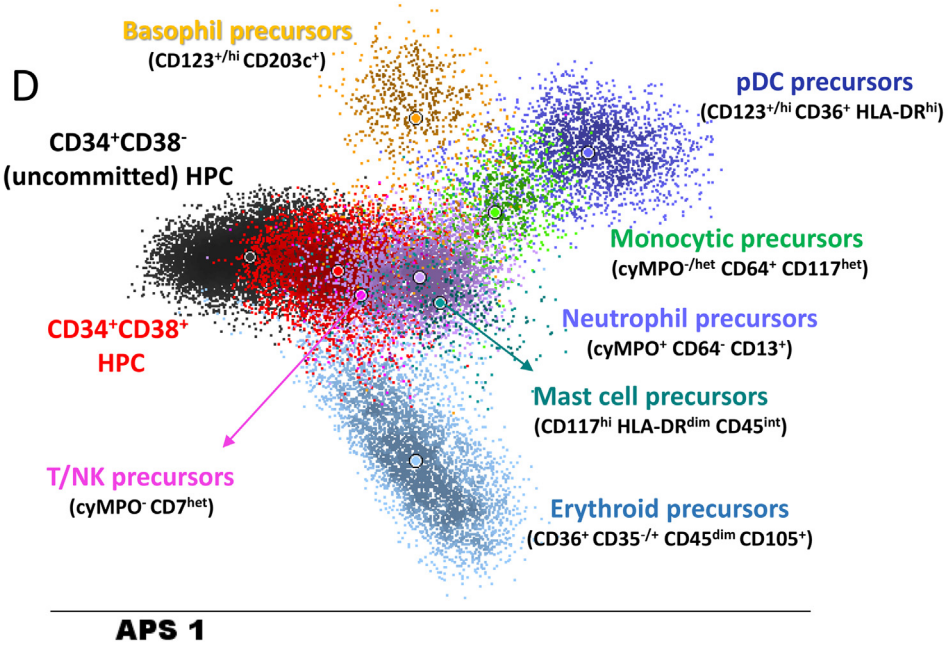

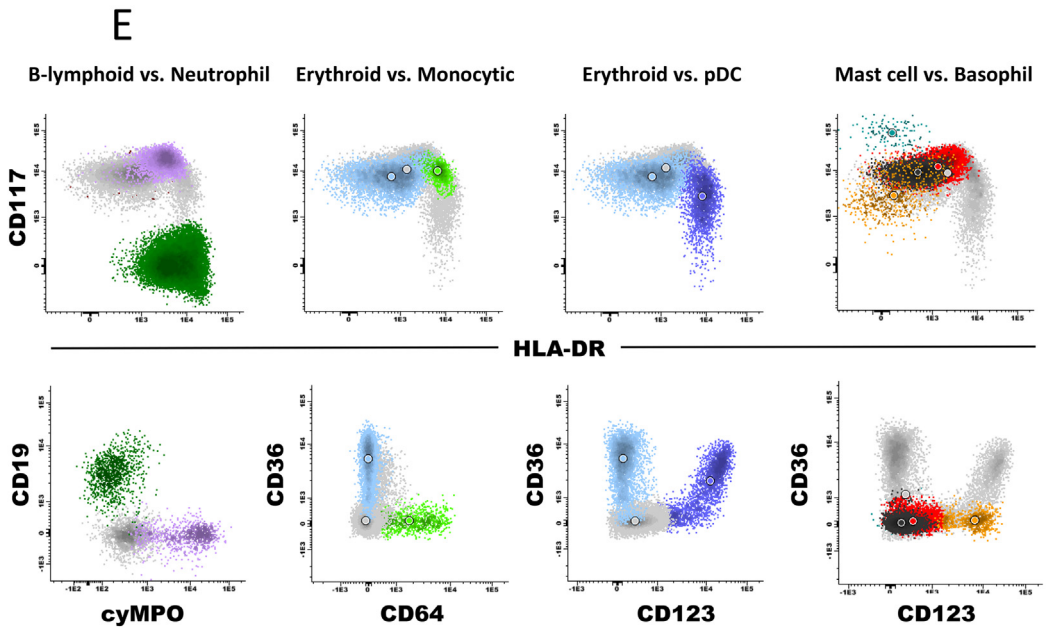

(caption on next page)

Fig. 1. Identification of bone marrow hematopoietic progenitor and precursor cells (HPC) based on CD34 (panel A) and CD45 expression profiles (panel B) and the main subpopulations of $CD34^+$ $CD73^+$ endothelial cells (red dots), $CD73^-CD19^-$ myeloid and $CD73^-CD19^+$ B-lymphoid (blue and green dots, respectively) $CD34^+$ HPC (panel C). Panel D depicts the relative distribution and phenotypic profile of $CD34^+$ HPC in a representative BM sample, including both uncommitted (black dots) and committed precursors to the B- and T/NK lymphoid lineages (pink dots) and the different myeloid cell lineages in a single automatic population separator (APS 1) diagram based on supervised principal component analysis (PC1 is shown on the X-axis and PC2 on the Y axes) (panel D). In panel E, bivariate dot plot histograms illustrating the specific phenotypes of the distinct subsets of $CD34^+$ precursors, are shown. pDC, plasmacytoid dendritic cell. (For interpretation of the references to color in this figure legend, the reader is referred to the web version of this article.)

minor myeloid cell compartments. Thus, differentiation of $CD34^+$ toward pDC represents between 1 and 9% of all BM $CD34^+$ cells. Differentiation of $CD34^+$ HPC to pDC is associated with acquisition of (strong) reactivity for the IL-3 receptor α-chain ($CD123^{+/hi}$) (Fig. 1D-E) and $HLADR^{hi}$, followed by positivity for CD36 and CD4 (Matarraz et al., 2008; Martin-Martin et al., 2009; Olweus et al., 1997) (Table 1). In turn, mast cell- and basophil-lineage committed $CD34^+$ precursors (each represents < 1% of all BM $CD34^+$ cells) show early acquisition of the NPP-3 molecule $CD203c^+$ together with loss of HLA-DR ($HLADR^{lo/-}$) and increased vs. decreased reactivity for CD117, respectively (Matarraz et al., 2008; Teodosio et al., 2015; Teodosio et al., 2010) (Table 1 and Fig. 1D–E). Although expression of cyEPO specifically identifies differentiation of BM cells toward the eosinophil lineage, no $cyEPO^+$ cells have been identified so far among normal BM $CD34^+$ BM precursors (Matarraz et al., 2008) (Table 1). Similarly, reliable identification of $CD34^+$ megakaryocytic precursors in normal BM also remains a challenge. In part, this is due to their low frequency, the relatively limited availability of megakaryocytic-associated markers and the fact that most of them also stain platelets. Altogether, this translates into artifact quantification of BM $CD34^+$ megakaryocytic precursors (Table 1) (Matarraz et al., 2008; Matarraz et al., 2010; Damasceno et al., 2016; Veglia et al., 2018). Likewise, identification of $CD34^+$ precursors committed to other myeloid cells, including myeloid DC (mDCs) or myeloid suppressor cell lineages (MySCs) still remains a challenge (Damasceno et al., 2016; Veglia et al., 2018).

Finally, around one third of all BM $CD34^+$ cells show commitment to the B-lymphoid lineage ($CD34^+$ $nuTdT^+$ $cyCD79a^{-/+}$ $CD19^{-/+}$ $CD10^{-/+}$; 20–25%) and to a lesser extent also, to the T/NK/DC lineages ($CD34^+$ $CD7^+$; 10–15%) (Theunissen et al., 2017b; Matarraz et al., 2008; Matarraz et al., 2010) (Table 1; Fig. 1D–E). Of note, the percentage of B-lymphoid precursors within BM $CD34^+$ HPC varies significantly throughout life, higher numbers being observed within the first years of life with a significant decrease in their proportion at puberty (Lucio et al., 1999; Rossi et al., 2005).

3. Myeloid maturation in the bone marrow

Once $CD34^+$ cell precursors committed to the main myeloid cell lineages are identified, their subsequent differentiation pathways can be easily delineated among maturing $CD34^-$ BM cells (Fig. 2). In turn, identification of early precursors corresponding to cell populations with uncertain ontogenic origin and variable phenotypic characteristics (e.g. MySCs) remains troublesome (Veglia et al., 2018).

4. Erythroid maturation

In BM smears, erythroid cells typically vary between 2% and 30% of the whole BM cellularity (Matarraz et al., 2008; Matarraz et al., 2010) (Table 1). Such variable distribution of erythroid precursors is due to with a combination of technical and biological variables. Among others, these include a variable degree of sample hemodilution, the use of distinct lysing reagents used and/or the intrinsic biological heterogeneity of this cell compartment (Delgado et al., 2017). Despite this variability, erythroid maturation stages can be clearly defined on phenotypic grounds in BM. Thus, early BM erythroid precursors mostly corresponding to pro-erythroblasts (i.e. $CD34^+$ $CD105^+$ $CD36^+$), rapidly loose expression of CD34 and HLADR, CD117, CD13 and CD33. In parallel, they acquire low levels of CD173, CD238 and reactivity for the

Table 1
Distribution and immunophenotypic patterns of major and minor $CD34^+$ and/or $CD117^+$ cell compartments of human bone marrow myeloid and lymphoid cells.

$CD34^+$ cell compartment	Phenotype	Distribution (%)
% BM $CD34^+$ precursor cells		0.9% (0.2–1.6)
Myeloid precursors	$CD38^+$ $CD45^{lo}$ $CD117^+$ $HLA\text{-}DR^{het}$	77% (57–85%)
Neutrophil lineage	$cyMPO^+$ $CD64^-$ $CD13^+$	33% (26–38%)
Erythroid lineage	$CD36^+$ $CD35^{-/+}$ $CD45^{lo}$ $CD105^+$	35% (24–37%)
Monocytic lineage	$cyMPO^{-/het}$ $CD64^+$ $CD117^{het}$	22% (16–28%)
pDC lineage	$CD123^{+/hi}$ $CD36^+$ $CD45^{lo}$ $HLA\text{-}DR^{hi}$	6% (1–9%)
Basophil lineage	$CD123^{+/hi}$ $CD45^+$ $CD117^{lo}$ $HLA\text{-}DR^{lo}$ $CD203c^+$	< 1% (0–3%)
Megakaryocytic lineage	$CD61^+$ $CD45^{lo}$ $CD203c^{lo}$	< 1%
Eosinophil lineage	$cyMPO^-$ CD15/$CD65^+$ $cyEPO^+$	< 1%
Mast cell lineage	$CD117^{hi}$ $HLA\text{-}DR^{lo}$ $CD45^{int}$	< 1%
B-lymphoid precursors	$nuTdT^+$ $cyCD79a^+$ $CD19^+$	23% (< 1–45%)
T/NK/DC precursors	$cyMPO^-$ $CD7^{het}$	12% (10–15%)
% BM $CD34^-CD117^+$ myeloid precursors		2.3% (0.8–2.7%)
Neutrophil precursors	$cyMPO^{hi}$ $HLA\text{-}DR^{het}$ $CD13^{hi}$	54.6% (53–69%)
Erythroid precursors	$cyMPO^-$ $HLA\text{-}DR^{het}$ $CD105^+CD36^{hi}$	30% (21–40%)
Monocytic precursors	$cyMPO^+$ $HLA\text{-}DR^{hi}$ $CD13^{int}$ $CD64^{+/hi}$ $CD14^-$	10% (5–16%)
$CD34^-CD117^-$ maturing myeloid cells		
Neutrophil lineage	$cyMPO^{lo}$ $HLA\text{-}DR^-$ $CD13^{het}$	59% (46–74%)
Erythroid lineage	$cyMPO^-$ $HLA\text{-}DR^-$ $CD105^-CD36^{hi}$	15% (2–29%)
Monocytic lineage	$cyMPO^+$ $HLA\text{-}DR^{hi}$ $CD64^{hi}$ $CD14^{het}$	4% (2–6%)
pDC lineage	$CD123^{hi}$ $CD36^+$ $CD45^{lo}$ $HLA\text{-}DR^{hi}$	0.2% (0–0.6%)
Basophil lineage	$CD123^{hi}$ $CD45^+$ $HLA\text{-}DR^-$ $CD203c^+$	0.4% (0.05–3%)
Eosinophil lineage	$cyMPO^-$ CD15/$CD65^+$ $cyEPO^+$	2.3% (0–4%)
Mast cell lineage	$CD117^{hi}$ $HLA\text{-}DR^-$ $CD45^{int}$	0.005% (0–0.02%)

Results expressed as percentage (median and range) of all bone marrow (BM) cells or as percentage of the parent population category used as denominator. pDC, plasmacytoid dendritic cell. Het, heterogeneous expression; hi, high expression; lo, low expression; int, intermediate expression levels.

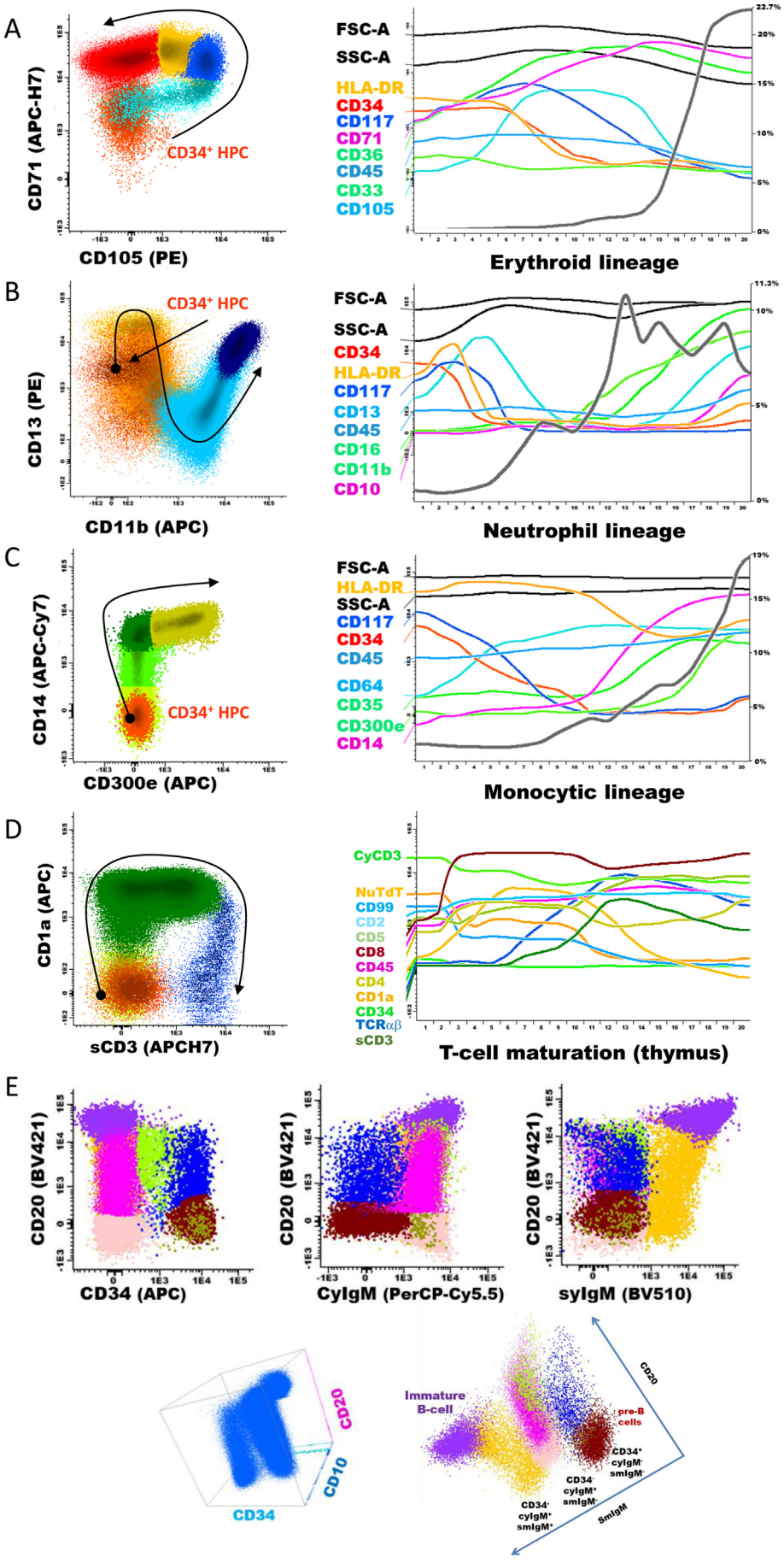

Fig. 2. Immunophenotypic patterns of distinct hematopoietic cell compartments in BM based on EuroFlow panels. Marker combinations were validated as showing an optimal performance for dissecting multiple maturation pathways. In each panel (panels A–D), arrows represent the maturation pathway from immature $CD34^+$ hematopoietic progenitor and precursor cells (HPC; orange dots) to maturing/mature (i.e. $CD34^-$) cells, per cell lineage. Dissection of the distinct maturation patterns of erythroid (panel A; BM), neutrophil (panel B; BM), monocytic (panel C; BM), T-cell (panel D; thymus) and B-cell (panel E; BM) precursors is represented on bivariate dot plot histograms (panels A–D, left column) and maturation diagrams (panels A–D, right column). Color lines represent the level of expression of markers corresponding to each maturation stage. Grey lines represent the percentage of events within each maturation stage. Twenty maturation stages were defined by default for smooth graphical representation along the maturation pathway of each cell lineage. Of note, more than one maturation pathway is observed during B-cell differentiation in the BM (panel E). Thus, a subset of BM $CD34^+$ B-cell precursors can be identified, which already shows $cyIg\mu^+$ expression, while other $CD10^+$ $CD34^+$ B-cell precursors depict similar $CD20^+$ levels, associated with heterogeneous expression of CD34, cyIgμ and also sIgM/k and sIgM/λ. Based on these apparently asynchronous profile, a few clearly distinct B-cell maturation pathways can be visualized based on CD20, CD34 and cyIgμ expression profiles. Maturation of T-cell precursors depicted in panel D is shown in the absence of CD4 and CD8 staining, which explains why there is no split into the $CD4^+CD8^-$ and $CD8^+CD4^-$ thymic T-cell precursor pathways.

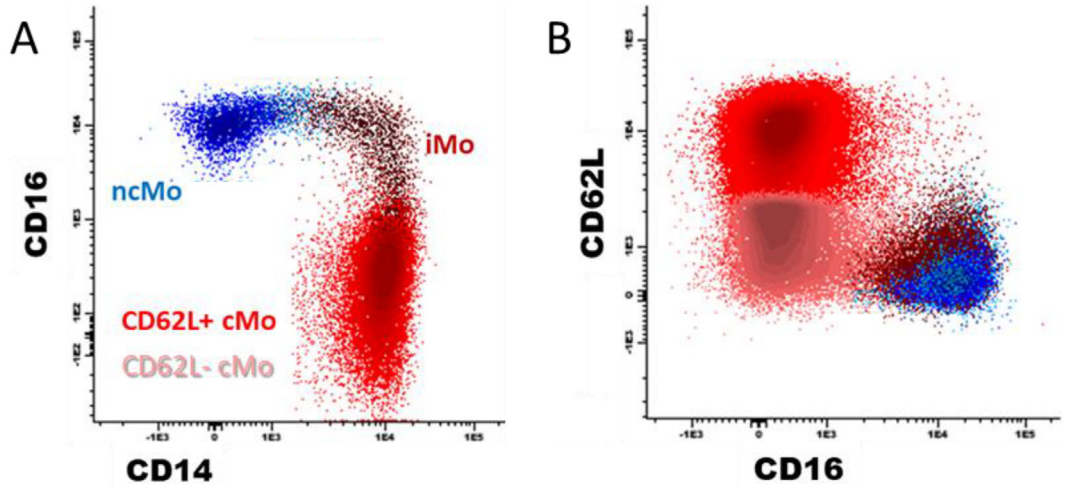

Fig. 3. Identification of distinct subsets of monocytes in peripheral blood by the expression levels of CD14 and/or CD16. Panel A: classical monocytes (cMo; $CD14^{hi}$ $CD16^{-}$ red colored events) are clearly discriminated from intermediate ($CD14^{hi}$ $CD16^{+}$ brown colored events) and non-classical monocytes (ncMo; $CD14^{-/lo}$ $CD16^{+}$ blue colored events). Panel B depicts the subsets of classical $CD62L^{-}$ vs. $CD62L^{+}$ monocytes (red colored events). (For interpretation of the references to color in this figure legend, the reader is referred to the web version of this article.)

Coxsackie-adenovirus receptor (CAR) protein, together with increasing levels of the transferrin receptor (i.e. $CD71^{+/hi}$) (Fig. 2A) (Machherndl-Spandl et al., 2013). Morphologically, these erythroid precursors correspond to basophilic erythroblasts (Loken et al., 1987a; Westers et al., 2017; Kalina et al., 2012; Laranjeira et al., 2015; Rebel et al., 2000). Further erythroid maturation is linked to upregulation of glycophorin A ($CD235a^{+}$), $CD173^{+}$, $CD233^{+}$, $CD238^{+}$ and $CD239^{+}$, associated with loss of CD105 expression. This erythroid phenotypic stage defines the transition from polychromatophilic to orthochromatic erythroblasts (Fig. 2A) (Loken et al., 1987a; Westers et al., 2017; Kalina et al., 2012; Laranjeira et al., 2015; Machherndl-Spandl et al., 2013; Rebel et al., 2000). Finally, during cell enucleation erythroid precursors simultaneously loose CD36 and CD71 expression, giving rise to $CD36^{-}$ $CD71^{-}$ reticulocytes and mature erythrocytes (Fig. 2A) (Loken et al., 1987a; Westers et al., 2017; Kalina et al., 2012; Laranjeira et al., 2015; Rebel et al., 2000). Both types of erythroid cells enter the blood stream for oxygen transportation to tissues across the body and both detoxification and elimination of immune complexes throughout the entire organism (Mello et al., 2017).

5. Neutrophil maturation

Neutrophils play a key role in eliminating pathogens (Summers et al., 2010). In steady state healthy subjects, neutrophil lineage cells represent around 46%–74% of the whole BM cellularity (Table 1) (Matarraz et al., 2008; Matarraz et al., 2010). As described above, early neutrophil precursors can be recognized by co-expression of $cyMPO^{+}$, $CD34^{+}$, $CD13^{hi}$ and $CD33^{hi}$ (Matarraz et al., 2008; Matarraz et al., 2010). These precursors, progressively acquire higher $cyMPO^{+/hi}$ levels, together with expression of $CD15^{+/hi}$ and $CD65^{+/hi}$. At this stage, neutrophil precursors sequentially downregulate CD34 (at the myeloblast stage), HLADR (in the transition between myeloblasts and promyelocytes), CD117 (from the promyelocyte to the myelocyte stage) and finally also, CD13 expression (at the myelocyte stage) (Fig. 2B) (van Dongen et al., 2012; Matarraz et al., 2008; Matarraz et al., 2010). In addition, maturing neutrophil precursors sequentially acquire surface membrane expression of distinct functional molecules. These include: i) the CD11b integrin/complement receptor on myelocytes; ii) the CD16 low-affinity IgG receptor in the transition from the myelocyte to metamyelocytes stage and later on, iii) both the CD13 (re-expressed on metamyelocytes) and iv) CD10 endopeptidases (from bands to segmented neutrophils) (Fig. 2B) (van Dongen et al., 2012; Matarraz et al., 2008; Matarraz et al., 2010). Finally, mature $CD11b^{hi}$ $CD16^{hi}$ $CD13^{hi}$ $CD10^{+}$ neutrophils and a minor fraction of their immediate precursors (bands) reach PB where they persist for a limited lifetime (around 24–72 h). However, under specific circumstances, mature neutrophils can eventually be chemo-attracted during an inflammatory process, toward inflamed tissues. Under such inflammatory conditions, mature neutrophils and bands are actively recruited from the BM into PB due to massive tissue demand, leading to abnormally high counts of left-shifted circulating neutrophils (Summers et al., 2010).

6. Monocytic maturation

Monocytic cells comprise a range of functionally distinct subpopulations that can be phenotypically recognized with comprehensive antibody combinations (Damasceno et al., 2019). Co-expression of $CD34^{+}$ and $CD64^{+}$ defines early HPC commitment toward the monocytic lineage in BM (Matarraz et al., 2008; Matarraz et al., 2010; Matarraz et al., 2017). At this stage, early monocytic precursors (i.e. monoblasts) show heterogeneous CD64 expression levels, while they progressively loose HPC-associated markers such as CD34 and (immediately after) CD117. Monoblasts upregulate additional myeloid/monocytic markers such as CD11c, cyLysozyme, cyCD68 followed by CD36 and CD35 (van Dongen et al., 2012; Matarraz et al., 2017; Dunphy, 2011). Further maturation of monoblasts is associated with sequentially greater levels of CD11b, CD14 (from monoblasts to promonocytes), and both CD300e and CD312 (from promonocytes to mature monocytes) (Fig. 2C) (Matarraz et al., 2017). Both immature (e.g. $CD64^{hi}CD14^{-}$) and mature (e.g. $CD300e^{hi}$) monocytic cells show expression of L-selectin ($CD62L^{+}$), while presence vs. absence of expression of this marker defines distinct maturation-associated subsets of monocytes in PB and lymphoid tissues (Damasceno et al., 2019).

In contrast to PB neutrophils, circulating monocytes show a high phenotypic heterogeneity (Damasceno et al., 2019). Hence, three main populations of mature monocytes have been recurrently described in PB: i) classical monocytes ($CD300e^{hi}$ $CD14^{hi}$ $CD16^{-}$), ii) intermediate monocytes ($CD300e^{hi}$ $CD14^{hi}$ $CD16^{+}$) and, iii) non-classical monocytes ($CD300e^{hi}$ $CD14^{lo/-}$ $CD16^{+}$) (Fig. 3A) (Damasceno et al., 2016; Ziegler-Heitbrock et al., 2010). Among classical monocytes, additional subsets have been identified based on the expression of CD62L and the high affinity IgE receptor (FcεRI). Thus, $CD62L^{+}$ monocytes predominate in PB, while those lacking CD62L are more frequent in secondary lymphoid tissues (Fig. 3B) (Damasceno et al., 2019).

7. Maturation of plasmacytoid dendritic cells

Dendritic cells correspond to the major population of specialized antigen-presenting cells responsible for priming T-cells (Eisenbarth, 2019). In BM, early commitment of $CD34^+$ hematopoietic precursors to the pDC lineage is phenotypically associated with a $CD117^+$ $CD123^{hi}$ $HLADR^{hi}$ phenotype. Like for other BM cell compartments, maturation of pDC precursors is associated with downregulation of immature markers (first CD34 and subsequently CD117) (Martin-Martin et al., 2009). In parallel, pDC precursors acquire positivity for CD36 (Olweus et al., 1997; Almeida et al., 1999) followed by expression of $CD4^+$, $CD303^+$ and $CD304^+$ (i.e. neuropilin-1). This unique hematopoietic cell phenotype is restricted to mature BM and circulating pDC (Martin-Martin et al., 2009; Almeida et al., 1999). Moreover, these cells (partially or totally) express the CD22 and CD7 lymphoid-associated markers (Martin-Martin et al., 2009; Almeida et al., 1999).

8. Maturation toward the basophil lineage

The basophil lineage is among the least common granulocyte compartment with both pro- and anti-inflammatory functions (Schwartz et al., 2016). Despite many similarities exist between basophils and mast cells, basophil lineage cells complete their maturation process in BM. Thus, early basophil precursors are among $CD34^+$ $CD38^+$ $IL\text{-}3R\alpha^+$ $IL\text{-}5R\alpha^+$ $CD45RA^-$ myeloid progenitors. Subsequent differentiation toward the basophil lineage is characterized by increasing levels of CD123 expression ($CD123^{+/hi}$) and progressive loss of HLA-DR ($HLADR^{+/-}$). This leads to the unique $CD123^{hi}$ $HLADR^-$ $CD203c^+$ basophil phenotype (Matarraz et al., 2008). Other markers that are highly expressed by terminally differentiated basophils include $CD9^+$, $CD11b^+$, $CD22^+$, $CD25^{dim}$, $CD33^+$, $CD35^+$, CD40L, and CCR3 as well as $cy2D7^+$ (an intracellular protein characteristic of the basophil lineage), $Fc\varepsilon RI^+$ and $CD13^{-/lo}$. Such phenotype is retained by mature BM and circulating PB basophils (Han et al., 2008).

9. Mast cell differentiation

Similarly to basophil precursors and mature basophils, mast cell precursors also show a $CD203c^+$ phenotype associated with strong CD33 expression (Teodosio et al., 2015; Teodosio et al., 2013). In contrast, mast cell precursors already show very-high expression of CD117 at early stages (Matarraz et al., 2008; Mayado et al., 2018; Teodosio et al., 2015; Teodosio et al., 2013), even before acquisition of CD203c (Teodosio et al., 2015), while basophil differentiation is associated with down-regulation of CD117 ($CD117^{-/lo}$) (Fig. 1E) (Teodosio et al., 2015; Almeida et al., 1999; Teodosio et al., 2013). Thereafter, mast cell precursors acquire cytoplasmic expression of enzymes characteristic of mature mast cells, such as tryptase and carboxypeptidase. This is accompanied by upregulation of CD203c and FcεRI expression, two cell surface markers shared with basophils (Teodosio et al., 2015; Teodosio et al., 2013). Despite mast cell maturation occurs in the BM, $CD34^+$ $CD117^{hi}$ mast cell precursors can enter the PB circulation and migrate to distinct tissues and mucosa, including the BM (Mayado et al., 2018; Dahlin et al., 2017). At these tissues, mast cell precursors undergo terminal differentiation until they become mature mast cells, displaying heterogeneous phenotypes depending on their tissue destination (Teodosio et al., 2015; Teodosio et al., 2013). Due to the low frequency of mast cells in BM (median of < 0.01%) (Matarraz et al., 2008; Teodosio et al., 2015; Teodosio et al., 2013), it is rather difficult to detect all maturation stages described above in normal BM, where most mast cells show a mature resting phenotype. However, early mast cell maturation stages become evident in reactive and/or regenerating BM (e.g. after chemotherapy) (Teodosio et al., 2015; Teodosio et al., 2013).

10. Eosinophil and megakaryocytic differentiation

As for human basophils, in vitro eosinophil differentiation has been previously associated with $CD34^+$ $CD38^+$ $IL\text{-}3R\alpha^+$ $IL\text{-}5R\alpha^+$ $CD45RA^-$ myeloid progenitors, while megakaryocytic differentiation might derive from the $IL\text{-}5R\alpha^-$ precursor cell fraction (Mori et al., 2009). However, in human BM maturing eosinophil and megakaryocytic cells are phenotypically detectable only within the $CD34^-$ cell compartments. The maturation of these two cell lineages is associated with loss of CD34, CD117 and HLADR expression, together with co-expression of $CD11b^+$, $CD15^+$, $CD65^+$ and either $cyEPO^+$ (in the absence of CD16) or $CD61^+$, $CD41^+$ and $CD42^+$, respectively (Mori et al., 2009; Tomer, 2004; Tomer et al., 1989). Moreover, while mature eosinophils retain CD13, CD33 and CD45 expression, megakaryocytic maturation is associated with down-regulation and loss of these markers already at relatively early maturation stages (Mori et al., 2009; Tomer, 2004; Tomer et al., 1989).

11. Normal lymphoid maturation

Lymphoid precursors represent around 25%–30% of all BM $CD34^+$ cells (Matarraz et al., 2008; Matarraz et al., 2010). An early $CD34^+$ $CD10^+$ $CD45RA^+$ $CD19^-$ common lymphoid precursor has been identified in mice. However, the presence of a $CD34^+$ cell population displaying this specific phenotype, remains to be definitively demonstrated in primary human BM. Thus, human BM lymphoid precursors typically include two clearly distinct populations of $CD34^+$ $CD7^+$ T/NK precursors and $CD34^+$ $nuTdT^+$ B-cell precursors (Table 1, Fig. 1D–E) (Matarraz et al., 2008; Matarraz et al., 2010). In BM, B-cell precursors become immunocompetent B-lymphocytes via expression of immunoglobulins (Ig) on their cell surface (sIg^+). In contrast, both uncommitted and $CD34^+$ $CD7^+$ T-cell precursors migrate through PB to the thymus to complete their differentiation and maturation toward the distinct functional subpopulations of T-cells (Bhandoola et al., 2007).

12. T-cell maturation

Differentiation of $CD34^+$ $CD7^+$ $cyCD3^-$ precursors toward T-cells occurs in the thymus, through multiple sequential maturation stages. Hence, the more immature thymic precursors already co-express CD34, cyCD3, nuTdT and CD99, while they lack CD4, CD8 and surface membrane CD3. These cells initiate the rearrangement of T-cell receptor genes (TCR) (Fig. 2D) (Bhandoola et al., 2007; Baltanas et al., 2013). At this stage, T-lymphoid precursors also show $CD2^{lo}$ and $CD5^{lo}$ (Bhandoola et al., 2007; Baltanas et al., 2013). Later on, $CD34^-$ thymocytes progressively loose CD99 and nuTdT expression, while they upregulate expression of $CD1a^+$, $CD4^+$ and $CD8^+$. Thereby, they give rise to $CD4^+$ $CD8^+$ double-positive T-cell precursors (Fig. 2D) (Bhandoola et al., 2007; Baltanas et al., 2013). Further differentiation toward $CD4^+$ or $CD8^+$ T-lymphocytes is associated with a slight decrease of cyCD3 (from $cyCD3^{hi}$ to $cyCD3^+$) and CD1a levels (toward $CD1a^-$). This is accompanied by expression of the $CD3^+/TCR^+$ complex on the cell surface membrane and a mature $CD45^{hi}$, $CD5^{hi}$ and $CD2^{hi}$ T-cell phenotype (Fig. 2D) (Bhandoola et al., 2007; Baltanas et al., 2013).

Naïve $CD4^+$ and $CD8^+$ mature T-cells typically co-express $CD45RA^+$ and CCR7 $(CD197)^+$ (Baltanas et al., 2013). Once these cells had contacted with their specific antigen, they differentiate into: i) central memory (i.e. $CD45RA^-$ $CCR7^+$); ii) peripheral memory (i.e. $CD45RA^-$ $CCR7^-$); and, iii) effector (i.e. $CD45RA^+$ $CCR7^-$) T-cells (Larbi and Fulop, 2014; van der Burg et al., 2019; Mahnke et al., 2013). Of note, among memory and effector cells, flow cytometry immunophenotyping currently allows identification of multiple functional T-cell compartments (> 120 subsets) according to their differential phenotypes (Fig. 4A) (Mahnke et al., 2013). Therefore, based on their PB phenotypes, > 25 subpopulations of regulatory T-cells

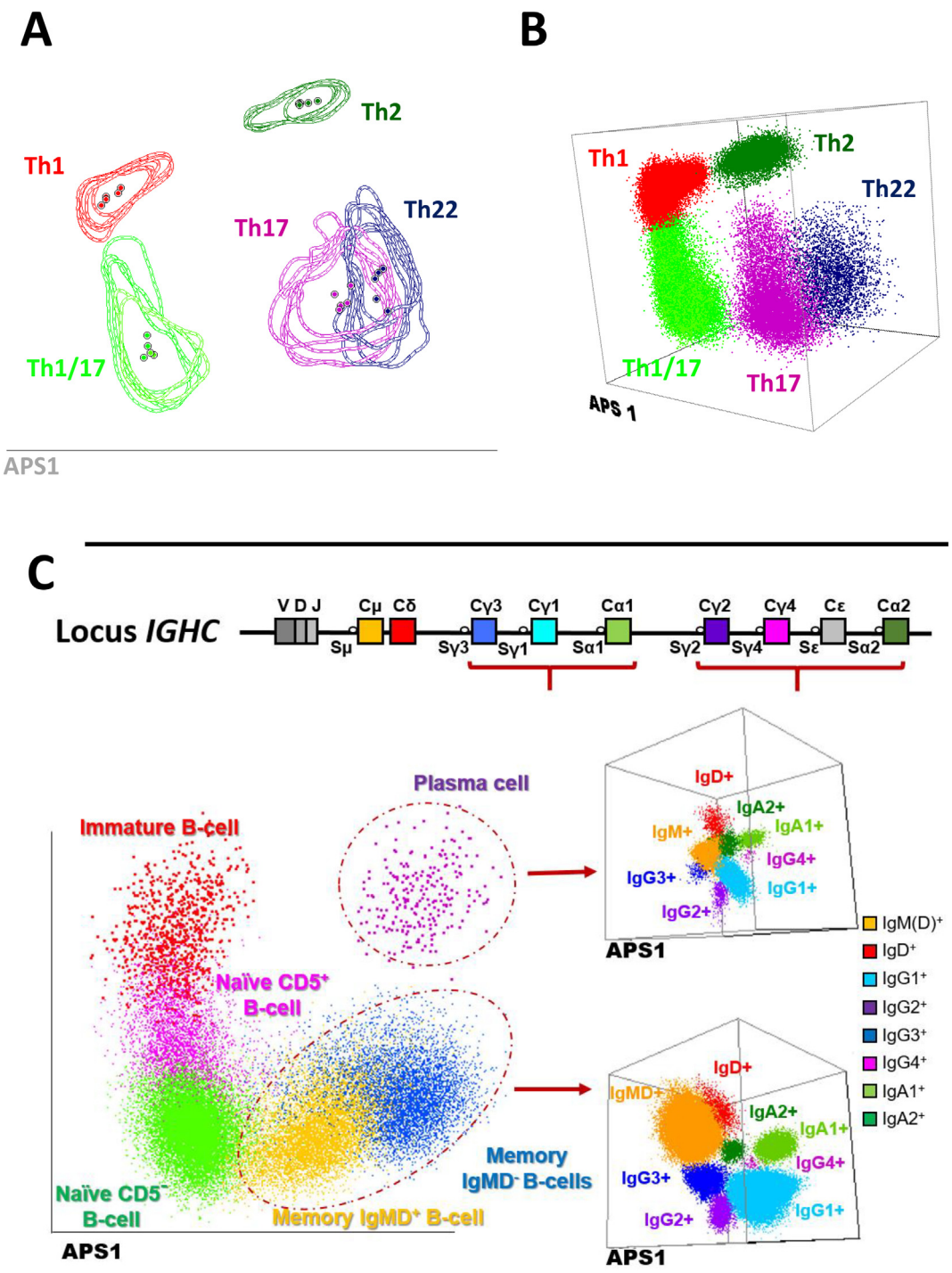

Fig. 4. Identification of distinct functional subsets of peripheral blood CD4$^+$ T-helper cells (panels A and B), B-cells and plasma cells (panel C) using combinations of markers designed by EuroFlow. Panel A shows a multidimensional view using principal component analysis (PCA; PC1 and PC2 shown in the X and Y-axis) of the main memory helper CD4$^+$ T-cell subsets (Th) from 5 peripheral blood samples: each individual circle and its corresponding contour line represent median fluorescence expression values for all immunophenotypic parameters and one standard deviation values, respectively, per sample. Total cell-events from the same Th cell-populations are shown in panel B, in a 3-dimensional plot of PC1 vs. PC3.

(FoxP3$^+$CD127$^-$CD25^{hi}CD39$^+$) can be identified at different maturation stages. Besides, Th1 (Tbet$^+$ CD183$^+$), Th2 (CD294$^+$CD194$^+$), Th17 (CD161$^+$CD194$^+$CD196$^+$) and Th22 (CD194$^+$ CD195$^+$ CCR10$^+$) memory helper T-cells, and multiple (> 65) subsets of follicular helper (Thf; CXCR5$^+$ CD279$^+$) and cytotoxic effector T-cells (cyPerforin$^+$ and/or cyGranzyme$^+$) are also recognizable in PB (Mahnke et al., 2013; Geginat et al., 2013; Maecker et al., 2012; Caramalho et al., 2015; Sallusto, 2016).

13. B-cell maturation

In contrast to T-cell development, differentiation of B-cell precursors toward immunocompetent B-lymphocytes occurs in BM (Loken et al., 1987b; Theunissen et al., 2017b). For decades, four different stages of B-cell maturation have been defined in human BM, which precede mature B-lymphocytes. These include: i) pro-B cells (nuTdT$^+$ cyCD79a$^+$ CD22$^+$ HLADR$^+$ CD34$^+$ CD38^{hi} CD10$^-$ CD19$^-$); ii) Pre-B I

cells (nuTdT^{+} cyCD79a^{+} CD22^{+} HLADR^{+} CD34^{+} CD38^{hi} CD10^{hi} CD19^{+}); iii) large pre-B II cells (nuTdT^{-} cyCD79a^{+} CD22^{+} HLADR^{+} CD34^{-} CD38^{hi} CD10^{+} CD19^{+}); and, iv) small pre-B II cells (nuTdT^{-} cyCD79a^{+} CD22^{+} HLADR^{+} CD34^{-} CD38^{hi} CD10^{+} CD19^{+} CD20^{-} cyIgμ^{+} sIg^{-}) (Lhermitte et al., 2018; van Zelm et al., 2005). Subsequently, pre-B II precursors differentiate toward immature/transitional B-lymphocytes, as reflected by progressive loss of CD38^{lo} and CD10^{lo}, together with expression of CD20^{hi}, CD5^{+} and sIgM^{+}, and progressively higher levels of sIgD$^{-/+}$. At more advanced stages of maturation, a fully mature and naïve B-cell phenotype is acquired (i.e. nuTdT^{-} cyCD79a^{+} CD22^{hi} HLADR^{+} CD34^{-} CD38$^{-/lo}$ CD10^{-} CD19^{+} CD20^{+} sIgM^{+}D^{+} CD5^{-}) (Blanco et al., 2018; van Zelm et al., 2005).

Despite the predominance of the above described B-cell maturation phenotypes, recent studies demonstrate the potential existence of divergent B-cell differentiation pathways (van der Burg et al., 2019). Occurrence of parallel B-cell maturation pathways would contribute to explain current discrepancies on the expression of several antigens along the classical B-cell maturation, such as CD34, nuTdT, CD20 and cyIgμ (Fig. 2E) (Theunissen et al., 2017b). For example, a subset of BM cyIgμ^{+} B-cell precursors have been identified among CD34^{+}CD10^{+} cells. In contrast, most other CD34^{+}CD10^{+} B-cell precursors are cyIgμ^{-} (Fig. 2E) (Theunissen et al., 2017b). Similarly, among CD20^{+} B-cell precursors, expression of CD34 and cyIgμ might be either negative or positive, with two clearly defined and distinct maturation pathways. The precise biological and clinical relevance of these distinct B-cell maturation pathways remains to be established.

Naïve B-lymphocytes (i.e. CD10^{-} CD38$^{-/lo}$ CD5^{-} CD27^{-} sIgM^{+}D^{+}) and immature/transitional B-lymphocytes (i.e. CD10^{lo} CD38^{+} CD5^{+} CD27^{-} sIgM^{+}D$^{-/+}$) enter the PB to reach secondary lymphoid tissues (Fig. 4B) (Perez-Andres et al., 2010; Perez-Andres et al., 2011; Sims et al., 2005; Lee et al., 2009). After antigen recognition, either inside or outside the germinal center (GC), CD10^{-} CD44^{hi} CD38$^{-/lo}$ naïve B-cells sequentially differentiate into CD10^{+} CD44^{lo} CD38^{hi} (Kjeldsen et al., 2011) B-cells and both antibody-secreting plasmablasts (i.e. CD19^{+} CD45^{+} CD38^{hi} CD27^{+} CD20$^{-/lo}$ CD138$^{-/lo}$) (Caraux et al., 2010) and memory B-cells (MBC) (most frequently CD38$^{-/lo}$ CD27^{+} CD20^{hi}) (Maecker et al., 2012; Berkowska et al., 2011). The latter two cell populations might have undergone or not heavy chain isotype and subclass switching from IgM^{+}D^{+} to IgG$_{1-4}$$^{+}$, IgA$_{1-2}$$^{+}$ or, to a lesser extent, IgE^{+} plasmablasts and memory B-cells (Fig. 4B) (Blanco et al., 2018; van Zelm et al., 2005; Blanco et al., 2019). This translates into up to 21 different subtypes of plasmablasts and MBC (11 and 10 subtypes, respectively) according to their maturation stage and the Ig-isotype and Ig-subclass they express (Blanco et al., 2018). Recently produced CD38^{hi} CD19^{+} CD45^{+} CD20$^{-/+het}$ CD138$^{-/+}$ VS38c$^{-/+}$ sIg$^{-/+}$ cyIg^{+} plasmablasts (Caraux et al., 2010; Paiva et al., 2011), enter the blood circulation from secondary lymphoid tissues, where they have been produced. After few days they migrate back to the BM, where they complete their differentiation toward long-living PC (i.e. CD19^{-} CD22^{-} CD20^{-} CD45^{lo} CD81^{+} CD27^{+} CD56$^{-/+}$ sIg^{-} cyIg^{+}) (Halliley et al., 2015). In turn, MBC recirculate between PB and secondary lymphoid tissues during a relatively longer period (months to years). Of note, both naïve B-cell and MBC populations might also be subclassified into: i) the major populations of CD21^{+} and CD27^{+} cells; and, ii) the minor subsets of cells lacking either one or both proteins. The functional role of these minor B-cell population remains to be fully elucidated (Blanco et al., 2018; van Zelm et al., 2005).

14. Aberrant phenotypes associated with clonal hematological disorders

At present it is well established that tumor hematopoietic cells mimic the phenotypic features of their corresponding normal counterpart. However, tumor cells systematically show phenotypic deviations/alterations from normal antigen expression profiles (Orfao et al., 1999). Such leukemia/lymphoma-associated aberrant phenotypes may derive from: i) minor normal phenotypes that remain undetectable in normal samples from healthy subjects (due to their low frequency); ii) cellular phenotypes which are absent in a given (normal) tissue; iii) altered phenotypic profiles due to underlying genetic lesions of tumor cells; or iv) phenotypic changes induced by interactions of tumor cells with their microenvironment (Orfao et al., 1999; Szczepanski et al., 2001).

At present, aberrant phenotypes of hematopoietic tumor cells are usually subclassified according to the patterns of deviation of antigen expression vs. normal phenotypes. These include: i) asynchronous antigen expression (i.e. either absence or expression of markers that should be present during normal hematopoiesis in the same or distinct stages of maturation, respectively); ii) abnormally decreased (under-expression) or increased (over-expression) reactivity for an individual marker in a given cell population; iii) mixed-lineage phenotypes defined by co-expression on individual tumor cells of two or more markers from different lineages; and, iv) ectopic phenotypes, as reflected by tumor-associated phenotypic profiles that correspond to a different tissue in healthy subjects (Orfao et al., 1999; Szczepanski et al., 2001; Schuurhuis et al., 2018). The presence of asynchronous maturation profiles is by far the most frequent aberrant phenotype observed in clonal hematopoietic cells. Conversely, mixed-lineage phenotypes represent the most reliable aberrant patterns to identify tumor cells, as they are typically related to (clonal) neoplastic conditions.

From a practical point of view, specific detection of tumor cells by flow cytometry based on their aberrant phenotypes is of great clinical utility, particularly for minimal disease detection, either at diagnosis or after starting therapy. In addition, some aberrant phenotypes of hematopoietic tumor cells are strongly associated with underlying genetic/molecular alterations (Orfao et al., 1999), and might be used as surrogate markers to direct further molecular analyses.

Acknowledgements

This work has been partially supported by the following grants: RTICC RD12/0036/0048-FEDER, Biomedical Research Networking Center Consortium- CIBER-CIBERONC (CB16/12/00400 - FEDER), PI16/00787-FEDER, from the Instituto de Salud Carlos III (ISCIII), Ministerio de Economía y Competitividad, Madrid, Spain.

The contents of this paper have been previously published in Spanish language in (Muñoz Calleja and Minguela, 2019) and permission of both the authors and the Publisher (Elsevier) were obtained to publish this English updated version of the manuscript.

References

Almeida, J., Bueno, C., Alguero, M.C., Sanchez, M.L., Canizo, M.C., Fernandez, M.E., et al., 1999. Extensive characterization of the immunophenotype and pattern of cytokine production by distinct subpopulations of normal human peripheral blood MHC II + /lineage-cells. Clin. Exp. Immunol. 118 (3), 392–401.

Angelos, M.G., Abrahante, J.E., Blum, R.H., Kaufman, D.S., 2018. Single cell resolution of human hematoendothelial cells defines transcriptional signatures of hemogenic endothelium. Stem Cells 36 (2), 206–217.

Baltanas, F.C., Perez-Andres, M., Ginel-Picardo, A., Diaz, D., Jimeno, D., Liceras-Boillos, P., et al., 2013. Functional redundancy of Sos1 and Sos2 for lymphopoiesis and organismal homeostasis and survival. Mol. Cell. Biol. 33 (22), 4562–4578.

Berkowska, M.A., Driessen, G.J., Bikos, V., Grosserichter-Wagener, C., Stamatopoulos, K., Cerutti, A., et al., 2011. Human memory B cells originate from three distinct germinal center-dependent and -independent maturation pathways. Blood. 118 (8), 2150–2158.

Bhandoola, A., von Boehmer, H., Petrie, H.T., Zuniga-Pflucker, J.C., 2007. Commitment and developmental potential of extrathymic and intrathymic T cell precursors: plenty to choose from. Immunity. 26 (6), 678–689.

Blanco, E., Perez-Andres, M., Arriba-Mendez, S., Contreras-Sanfeliciano, T., Criado, I., Pelak, O., et al., 2018. Age-associated distribution of normal B-cell and plasma cell subsets in peripheral blood. J. Allergy Clin. Immunol. 141 (6), 2208–2219 (e16).

Blanco, E., Perez-Andres, M., Arriba-Mendez, S., Serrano, C., Criado, I., Pino-Molina, L.D., et al., 2019. Defects in memory B-cell and plasma cell subsets expressing different immunoglobulin-subclasses in CVID and Ig-subclass deficiencies. J. Allergy Clin. Immunol. 144 (3), 809–824.

Busch, K., Klapproth, K., Barile, M., Flossdorf, M., Holland-Letz, T., Schlenner, S.M., et al.,

2015. Fundamental properties of unperturbed haematopoiesis from stem cells in vivo. Nature. 518 (7540), 542–546.
Caramalho, I., Nunes-Cabaco, H., Foxall, R.B., Sousa, A.E., 2015. Regulatory T-cell development in the human thymus. Front. Immunol. 6, 395.
Caraux, A., Klein, B., Paiva, B., Bret, C., Schmitz, A., Fuhler, G.M., et al., 2010. Circulating human B and plasma cells. Age-associated changes in counts and detailed characterization of circulating normal CD138- and CD138+ plasma cells. Haematologica. 95 (6), 1016–1020.
Chattopadhyay, P.K., Roederer, M., 2012. Cytometry: today's technology and tomorrow's horizons. Methods. 57 (3), 251–258.
Chattopadhyay, P.K., Gierahn, T.M., Roederer, M., Love, J.C., 2014. Single-cell technologies for monitoring immune systems. Nat. Immunol. 15 (2), 128–135.
Collin, M., Bigley, V., 2018. Human dendritic cell subsets: an update. Immunology. 154 (1), 3–20.
Dahlin, J.S., Ekoff, M., Grootens, J., Lof, L., Amini, R.M., Hagberg, H., et al., 2017. KIT signaling is dispensable for human mast cell progenitor development. Blood. 130 (16), 1785–1794.
Damasceno, D., Andres, M.P., van den Bossche, W.B., Flores-Montero, J., de Bruin, S., Teodosio, C., et al., 2016. Expression profile of novel cell surface molecules on different subsets of human peripheral blood antigen-presenting cells. Clin. Trans. Immunol. 5 (9), e100.
Damasceno, D., Teodosio, C., van den Bossche, W.B.L., Perez-Andres, M., Arriba-Mendez, S., Munoz-Bellvis, L., et al., 2019. Distribution of subsets of blood monocytic cells throughout life. J. Allergy Clin. Immunol. 144 (1), 320–323 (e6).
Delgado, J.A., Guillen-Grima, F., Moreno, C., Panizo, C., Perez-Robles, C., Mata, J.J., et al., 2017. A simple flow-cytometry method to evaluate peripheral blood contamination of bone marrow aspirates. J. Immunol. Methods 442, 54–58.
Dunphy, C.H., 2011. Comparative analysis of detecting monocytic cells and their aberrancy. Appl. Immunohistochem. Mol. Morphol. 19 (4), 336–340.
Eisenbarth, S.C., 2019. Dendritic cell subsets in T cell programming: location dictates function. Nat. Rev. Immunol. 19 (2), 89–103.
Flores-Montero, J., Sanoja-Flores, L., Paiva, B., Puig, N., Garcia-Sanchez, O., Bottcher, S., et al., 2017. Next generation flow for highly sensitive and standardized detection of minimal residual disease in multiple myeloma. Leukemia. 31 (10), 2094–2103.
Geginat, J., Paroni, M., Facciotti, F., Gruarin, P., Kastirr, I., Caprioli, F., et al., 2013. The CD4-centered universe of human T cell subsets. Semin. Immunol. 25 (4), 252–262.
Goardon, N., Marchi, E., Atzberger, A., Quek, L., Schuh, A., Soneji, S., et al., 2011. Coexistence of LMPP-like and GMP-like leukemia stem cells in acute myeloid leukemia. Cancer Cell 19 (1), 138–152.
Halliley, J.L., Tipton, C.M., Liesveld, J., Rosenberg, A.F., Darce, J., Gregoretti, I.V., et al., 2015. Long-lived plasma cells are contained within the CD19(−)CD38(hi)CD138(+) subset in human bone marrow. Immunity. 43 (1), 132–145.
Han, X., Jorgensen, J.L., Brahmandam, A., Schlette, E., Huh, Y.O., Shi, Y., et al., 2008. Immunophenotypic study of basophils by multiparameter flow cytometry. Arch. Pathol. Lab. Med. 132 (5), 813–819.
Kalina, T., Flores-Montero, J., van der Velden, V.H., Martin-Ayuso, M., Bottcher, S., Ritgen, M., et al., 2012. EuroFlow standardization of flow cytometer instrument settings and immunophenotyping protocols. Leukemia. 26 (9), 1986–2010.
Kjeldsen, M.K., Perez-Andres, M., Schmitz, A., Johansen, P., Boegsted, M., Nyegaard, M., et al., 2011. Multiparametric flow cytometry for identification and fluorescence activated cell sorting of five distinct B-cell subpopulations in normal tonsil tissue. Am. J. Clin. Pathol. 136 (6), 960–969.
Laranjeira, P., Rodrigues, R., Carvalheiro, T., Constanco, C., Vitoria, H., Matarraz, S., et al., 2015. Expression of CD44 and CD35 during normal and myelodysplastic erythropoiesis. Leuk. Res. 39 (3), 361–370.
Larbi, A., Fulop, T., 2014. From “truly naive” to “exhausted senescent” T cells: when markers predict functionality. Cytometry A 85 (1), 25–35.
Lee, J., Kuchen, S., Fischer, R., Chang, S., Lipsky, P.E., 2009. Identification and characterization of a human CD5+ pre-naive B cell population. J. Immunol. 182 (7), 4116–4126.
Lhermitte, L., Mejstrikova, E., van der Sluijs-Gelling, A.J., Grigore, G.E., Sedek, L., Bras, A.E., et al., 2018. Automated database-guided expert-supervised orientation for immunophenotypic diagnosis and classification of acute leukemia. Leukemia. 32 (4), 874–881.
Loken, M.R., Shah, V.O., Dattilio, K.L., Civin, C.I., 1987a. Flow cytometric analysis of human bone marrow: I. Normal erythroid development. Blood. 69 (1), 255–263.
Loken, M.R., Shah, V.O., Dattilio, K.L., Civin, C.I., 1987b. Flow cytometric analysis of human bone marrow. II. Normal B lymphocyte development. Blood. 70 (5), 1316–1324.
Lucio, P., Parreira, A., van den Beemd, M.W., van Lochem, E.G., van Wering, E.R., Baars, E., et al., 1999. Flow cytometric analysis of normal B cell differentiation: a frame of reference for the detection of minimal residual disease in precursor-B-ALL. Leukemia. 13 (3), 419–427.
Machherndl-Spandl, S., Suessner, S., Danzer, M., Proell, J., Gabriel, C., Lauf, J., et al., 2013. Molecular pathways of early CD105-positive erythroid cells as compared with CD34-positive common precursor cells by flow cytometric cell-sorting and gene expression profiling. Blood Cancer J. 3, e100.
Maecker, H.T., McCoy, J.P., Nussenblatt, R., 2012. Standardizing immunophenotyping for the human immunology project. Nat. Rev. Immunol. 12 (3), 191–200.
Mahnke, Y.D., Brodie, T.M., Sallusto, F., Roederer, M., Lugli, E., 2013. The who's who of T-cell differentiation: human memory T-cell subsets. Eur. J. Immunol. 43 (11), 2797–2809.
Majeti, R., Park, C.Y., Weissman, I.L., 2007. Identification of a hierarchy of multipotent hematopoietic progenitors in human cord blood. Cell Stem Cell 1 (6), 635–645.
Manz, M.G., Miyamoto, T., Akashi, K., Weissman, I.L., 2002. Prospective isolation of human clonogenic common myeloid progenitors. Proc. Natl. Acad. Sci. U. S. A. 99 (18), 11872–11877.
Martin-Martin, L., Almeida, J., Hernandez-Campo, P.M., Sanchez, M.L., Lecrevisse, Q., Orfao, A., 2009. Immunophenotypical, morphologic, and functional characterization of maturation-associated plasmacytoid dendritic cell subsets in normal adult human bone marrow. Transfusion. 49 (8), 1692–1708.
Matarraz, S., Lopez, A., Barrena, S., Fernandez, C., Jensen, E., Flores, J., et al., 2008. The immunophenotype of different immature, myeloid and B-cell lineage-committed CD34+ hematopoietic cells allows discrimination between normal/reactive and myelodysplastic syndrome precursors. Leukemia. 22 (6), 1175–1183.
Matarraz, S., Lopez, A., Barrena, S., Fernandez, C., Jensen, E., Flores-Montero, J., et al., 2010. Bone marrow cells from myelodysplastic syndromes show altered immunophenotypic profiles that may contribute to the diagnosis and prognostic stratification of the disease: a pilot study on a series of 56 patients. Cytometry B Clin. Cytom. 78 (3), 154–168.
Matarraz, S., Almeida, J., Flores-Montero, J., Lecrevisse, Q., Guerri, V., Lopez, A., et al., 2017. Introduction to the diagnosis and classification of monocytic-lineage leukemias by flow cytometry. Cytometry B Clin. Cytom. 92 (3), 218–227.
Matarraz, S., Leoz, P., Fernandez, C., Colado, E., Chillon, M.C., Vidriales, M.B., et al., 2018. Basophil-lineage commitment in acute promyelocytic leukemia predicts for severe bleeding after starting therapy. Modern Pathol. 31 (8), 1318–1331.
Mayado, A., Teodosio, C., Dasilva-Freire, N., Jara-Acevedo, M., Garcia-Montero, A.C., Alvarez-Twose, I., et al., 2018. Characterization of CD34(+) hematopoietic cells in systemic mastocytosis: potential role in disease dissemination. Allergy. 73 (6), 1294–1304.
Mello, F.V., Alves, L.R., Land, M.G., Teodosio, C., Sanchez, M.L., Barcena, P., et al., 2017. Maturation-associated gene expression profiles along normal human bone marrow monopoiesis. Br. J. Haematol. 176 (3), 464–474.
Mori, Y., Iwasaki, H., Kohno, K., Yoshimoto, G., Kikushige, Y., Okeda, A., et al., 2009. Identification of the human eosinophil lineage-committed progenitor: revision of phenotypic definition of the human common myeloid progenitor. J. Exp. Med. 206 (1), 183–193.
Muñoz Calleja, C., Minguela, Puras A., 2019. Diagnóstico y Monitorización Inmunofenotípica de las Neoplasias Leucocitarias Barcelona. Elsevier España, Spain.
Oguro, H., Ding, L., Morrison, S.J., 2013. SLAM family markers resolve functionally distinct subpopulations of hematopoietic stem cells and multipotent progenitors. Cell Stem Cell 13 (1), 102–116.
Olweus, J., BitMansour, A., Warnke, R., Thompson, P.A., Carballido, J., Picker, L.J., et al., 1997. Dendritic cell ontogeny: a human dendritic cell lineage of myeloid origin. Proc. Natl. Acad. Sci. U. S. A. 94 (23), 12551–12556.
Orfao, A., Schmitz, G., Brando, B., Ruiz-Arguelles, A., Basso, G., Braylan, R., et al., 1999. Clinically useful information provided by the flow cytometric immunophenotyping of hematological malignancies: current status and future directions. Clin. Chem. 45 (10), 1708–1717.
Paiva, B., Perez-Andres, M., Vidriales, M.B., Almeida, J., de las Heras, N., Mateos, M.V., et al., 2011. Competition between clonal plasma cells and normal cells for potentially overlapping bone marrow niches is associated with a progressively altered cellular distribution in MGUS vs myeloma. Leukemia. 25 (4), 697–706.
Pedreira, C.E., 2012. Automating flow cytometry. Cytometry A 81 (2), 110–111.
Pedreira, C.E., Costa, E.S., Lecrevisse, Q., van Dongen, J.J., Orfao, A., EuroFlow, C., 2013. Overview of clinical flow cytometry data analysis: recent advances and future challenges. Trends Biotechnol. 31 (7), 415–425.
Perez-Andres, M., Paiva, B., Nieto, W.G., Caraux, A., Schmitz, A., Almeida, J., et al., 2010. Human peripheral blood B-cell compartments: a crossroad in B-cell traffic. Cytometry B Clin. Cytom. 78 (Suppl. 1), S47–S60.
Perez-Andres, M., Grosserichter-Wagener, C., Teodosio, C., van Dongen, J.J., Orfao, A., van Zelm, M.C., 2011. The nature of circulating CD27+CD43+ B cells. J. Exp. Med. 208 (13), 2565–2566.
Rebel, V.I., Hartnett, S., Denham, J., Chan, M., Finberg, R., Sieff, C.A., 2000. Maturation and lineage-specific expression of the coxsackie and adenovirus receptor in hematopoietic cells. Stem Cells 18 (3), 176–182.
Rossi, D.J., Bryder, D., Zahn, J.M., Ahlenius, H., Sonu, R., Wagers, A.J., et al., 2005. Cell intrinsic alterations underlie hematopoietic stem cell aging. Proc. Natl. Acad. Sci. U. S. A. 102 (26), 9194–9199.
Sallusto, F., 2016. Heterogeneity of human CD4(+) T cells against microbes. Annu. Rev. Immunol. 34, 317–334.
Schuurhuis, G.J., Heuser, M., Freeman, S., Bene, M.C., Buccisano, F., Cloos, J., et al., 2018. Minimal/measurable residual disease in AML: consensus document from ELN MRD working party. Blood. 131 (12), 1275–1291.
Schwartz, C., Eberle, J.U., Voehringer, D., 2016. Basophils in inflammation. Eur. J. Pharmacol. 778, 90–95.
Sims, G.P., Ettinger, R., Shirota, Y., Yarboro, C.H., Illei, G.G., Lipsky, P.E., 2005. Identification and characterization of circulating human transitional B cells. Blood. 105 (11), 4390–4398.
Smadja, D.M., Cornet, A., Emmerich, J., Aiach, M., Gaussem, P., 2007. Endothelial progenitor cells: characterization, in vitro expansion, and prospects for autologous cell therapy. Cell Biol. Toxicol. 23 (4), 223–239.
Summers, C., Rankin, S.M., Condliffe, A.M., Singh, N., Peters, A.M., Chilvers, E.R., 2010. Neutrophil kinetics in health and disease. Trends Immunol. 31 (8), 318–324.
Szczepanski, T., Orfao, A., van der Velden, V.H., San Miguel, J.F., van Dongen, J.J., 2001. Minimal residual disease in leukaemia patients. Lancet Oncol. 2 (7), 409–417.
Teodosio, C., Garcia-Montero, A.C., Jara-Acevedo, M., Sanchez-Munoz, L., Alvarez-Twose, I., Nunez, R., et al., 2010. Mast cells from different molecular and prognostic subtypes of systemic mastocytosis display distinct immunophenotypes. J. Allergy Clin. Immunol. 125 (3), 719–726 (26 e1–26 e4).
Teodosio, C., Garcia-Montero, A.C., Jara-Acevedo, M., Sanchez-Munoz, L., Pedreira, C.E., Alvarez-Twose, I., et al., 2013. Gene expression profile of highly purified bone

marrow mast cells in systemic mastocytosis. J. Allergy Clin. Immunol. 131 (4), 1213–1224 (24 e1–4).
Teodosio, C., Mayado, A., Sanchez-Munoz, L., Morgado, J.M., Jara-Acevedo, M., Alvarez-Twose, I., et al., 2015. The immunophenotype of mast cells and its utility in the diagnostic work-up of systemic mastocytosis. J. Leukoc. Biol. 97 (1), 49–59.
Theunissen, P., Mejstrikova, E., Sedek, L., van der Sluijs-Gelling, A.J., Gaipa, G., Bartels, M., et al., 2017a. Standardized flow cytometry for highly sensitive MRD measurements in B-cell acute lymphoblastic leukemia. Blood. 129 (3), 347–357.
Theunissen, P.M.J., Sedek, L., De Haas, V., Szczepanski, T., Van Der Sluijs, A., Mejstrikova, E., et al., 2017b. Detailed immunophenotyping of B-cell precursors in regenerating bone marrow of acute lymphoblastic leukaemia patients: implications for minimal residual disease detection. Br. J. Haematol. 178 (2), 257–266.
Tomer, A., 2004. Human marrow megakaryocyte differentiation: multiparameter correlative analysis identifies von Willebrand factor as a sensitive and distinctive marker for early (2N and 4N) megakaryocytes. Blood. 104 (9), 2722–2727.
Tomer, A., Friese, P., Conklin, R., Bales, W., Archer, L., Harker, L.A., et al., 1989. Flow cytometric analysis of megakaryocytes from patients with abnormal platelet counts. Blood. 74 (2), 594–601.
van der Burg, M., Kalina, T., Perez-Andres, M., Vlkova, M., Lopez-Granados, E., Blanco, E., et al., 2019. The EuroFlow PID orientation tube for flow cytometric diagnostic screening of primary immunodeficiencies of the lymphoid system. Front. Immunol. 10, 246.
van Dongen, J.J., Lhermitte, L., Bottcher, S., Almeida, J., van der Velden, V.H., Flores-Montero, J., et al., 2012. EuroFlow antibody panels for standardized n-dimensional flow cytometric immunophenotyping of normal, reactive and malignant leukocytes. Leukemia. 26 (9), 1908–1975.
van Zelm, M.C., van der Burg, M., de Ridder, D., Barendregt, B.H., de Haas, E.F., Reinders, M.J., et al., 2005. Ig gene rearrangement steps are initiated in early human precursor B cell subsets and correlate with specific transcription factor expression. J. Immunol. 175 (9), 5912–5922.
Veglia, F., Perego, M., Gabrilovich, D., 2018. Myeloid-derived suppressor cells coming of age. Nat. Immunol. 19 (2), 108–119.
Westers, T.M., Cremers, E.M., Oelschlaegel, U., Johansson, U., Bettelheim, P., Matarraz, S., et al., 2017. Immunophenotypic analysis of erythroid dysplasia in myelodysplastic syndromes. A report from the IMDSFlow working group. Haematologica. 102 (2), 308–319.
Ziegler-Heitbrock, L., Ancuta, P., Crowe, S., Dalod, M., Grau, V., Hart, D.N., et al., 2010. Nomenclature of monocytes and dendritic cells in blood. Blood. 116 (16), e74–e80.